Received: 14 April 2020 | Revised: 19 June 2020 | Accepted: 10 July 2020

DOI: 10.1096/fj.202000886R

RESEARCH ARTICLE

THE FASEB JOURNAL

Mgs1 protein supports genome stability via recognition of G-quadruplex DNA structures

Theresa Zacheja[1] | **Agnes Toth**[2,3] | **Gabor M. Harami**[4] | **Qianlu Yang**[5,6] | **Eike Schwindt**[1] | **Mihály Kovács**[4,7] | **Katrin Paeschke**[1,5] | **Peter Burkovics**[2]

[1]Department of Oncology, Hematology and Rheumatology, University Hospital Bonn, Bonn, Germany

[2]Biological Research Centre, Institute of Genetics, Szeged, Hungary

[3]Doctoral School of Biology, Faculty of Science and Informatics, University of Szeged, Szeged, Hungary

[4]ELTE-MTA Momentum Motor Enzymology Research Group, Department of Biochemistry, Eötvös Loránd University, Budapest, Hungary

[5]Department of Biochemistry, Biocenter, University of Wuerzburg, Wuerzburg, Germany

[6]Department of Biochemistry and Molecular Biology, School of Basic Medical Sciences, Nanjing Medical University, Nanjing, China

[7]MTA-ELTE Motor Pharmacology Research Group, Department of Biochemistry, Eötvös Loránd University, Budapest, Hungary

Correspondence
Katrin Paeschke, Universitätsklinikum Bonn, Medizinische Klinik III, Venusberg-Campus 1, Gebäude 13, 3OG029 Bonn 53127, Hungary.
Email: katrin.paeschke@ukbonn.de

Peter Burkovics, Institute of Genetics, Biological Research Centre, Temesvari krt. 62, 6726 Szeged, Hungary.
Email: burkovics.peter@brc.hu

Funding information
Emmy-Noether Program of the Deutsche Forschungsgemeinschaft; EC | European Research Council (ERC), Grant/Award Number: 638988-G4DSB; NSFC | National Natural Science Foundation of China-Yunnan Joint Fund (NSFC-Yunnan Joint Fund), Grant/Award Number: 31700716; Nemzeti Kutatási, Fejlesztési és Innovációs Hivatal (NKFI Office), Grant/Award Number: 119361, 116072, ERC_HU117680 and 123989; Eötvös Loránd Tudományegyetem (ELTE), Grant/Award Number: 4.2.1/BOP 6072

Abstract

The integrity of the genetic material is crucial for every organism. One intrinsic attack to genome stability is stalling of the replication fork which can result in DNA breakage. Several factors, such as DNA lesions or the formation of stable secondary structures (eg, G-quadruplexes) can lead to replication fork stalling. G-quadruplexes (G4s) are well-characterized stable secondary DNA structures that can form within specific single-stranded DNA sequence motifs and have been shown to block/pause the replication machinery. In most genomes several helicases have been described to regulate G4 unfolding to preserve genome integrity, however, different experiments raise the hypothesis that processing of G4s during DNA replication is more complex and requires additional, so far unknown, proteins. Here, we show that the *Saccharomyces cerevisiae* Mgs1 protein robustly binds to G4 structures in vitro and preferentially acts at regions with a strong potential to form G4 structures in vivo. Our results suggest that Mgs1 binds to G4-forming sites and has a role in the maintenance of genome integrity.

KEYWORDS

DNA replication, genome stability, G-quadruplex, helicase, protein-DNA interaction

Abbreviations: BLM, bloom helicase; ChIP, chromatin immunoprecipitation; DSB, double strand break; EMSA, electrophoretic mobility-shift assay; FANCJ, Fanconi anemia group J protein; G4, G-quadruplex; GCR, gross chromosomal rearrangement; GST, glutathione S-transferase; HU, hydroxyurea; K_d, dissociation constant; Mgs1, maintenance of genome stability 1; MMS, methyl methanesulfonate; PCNA, proliferating cell nuclear antigen; Pif1, petite integration frequency protein 1; UV, ultraviolet; WRN, Werner helicase; WRNIP1, Werner interacting protein 1; YPD, yeast extract peptone dextrose; γH2A, phosphorylated H2A.

Theresa Zacheja and Agnes Toth contributed equally to this work.

Peter Burkovics and Katrin Paeschke contributed equally to this work.

1 | INTRODUCTION

Precise DNA replication is essential for the preservation of genome stability. DNA lesions, topological stress, nucleotide pool depletion, or stable secondary DNA structures are the major sources of replication stalling which can lead to DNA breaks and consequently genome instability.[1]

G-quadruplex (G4) structures are stable secondary DNA structures, which can be formed by Hoogsteen G-G base pairing within specific guanine-rich single-stranded (ss) DNA regions as reviewed in several publications.[2-4] In silico and in vitro studies have revealed that over 700 000 regions in the human genome have strong potential to fold into G4 structures.[5-8] Similarly, there are over 500 potential intrachromosomal G4 motifs in the *Saccharomyces cerevisiae* genome.[9,10] Different topologies of the G4 structure have been described in vitro (parallel, antiparallel, or hybrid); however, the biological relevance of these different conformations is not understood yet.[3,4] Regardless of topology, G4 structures were demonstrated to act as regulatory elements during transcription or telomere maintenance.[11-16] Additionally, due to their stability, G4 structures can challenge DNA replication and must be unfolded by proteins (eg, helicases).[17-19] In the absence of regulating proteins, the replication fork stalls at G4 motifs, leading to deletions or mutations.[20-24] Whereas the precise replication of G4 motifs is essential, it is not clear how the replication machinery recognizes these obstacles and how and why replication sometimes stalls approaching G4 motifs.[23,25,26] The most prominent group of G4 unfolding proteins are helicases.[19] Among the best characterized helicases, that unfold G4 DNA structures efficiently, are Pif1, Sgs1, and Hrq1 helicases in yeast,[22,23,27-31] and WRN, BLM, and FANCJ helicases in humans.[20,25,32,33] Mutation or deletion of these genes is linked to increased genome instability and is associated with elevated cancer risk in humans.[19,34-37] Nonetheless, the observed negative effects on genome stability in the absence of these helicases are not exclusively due to changes in G4 maintenance. Accumulating data suggest that specialized helicases act in the processing of G4 structures during specific processes (eg, Sgs1 unwinds G4 during transcription, and BLM inhibits recombination at G4 motifs in transcribed genes).[10,38] Based on the amount of potential G4 structures in most genomes and the lack of severe phenotypes in the absence of various individual helicases it has been suggested that members of the same protein family are able to compensate for each other's loss in G4 unfolding to some extent.[22] In *S. cerevisiae* there are two members of the RecQ family (Sgs1 and Hrq1), and one member of the Pif1 family (Pif1) which recognize G4 structures in vitro.[22-24,30,31,39,40] Although both helicase families function in the preservation of genome stability,[21,24] they have been implicated to regulate G4 structures during different processes. Sgs1 regulates G4 formation and, in turn influences transcription,[10,41] whereas Pif1 regulates G4 structures during S phase and supports DNA replication and prevents genome instability (mutations, deletions).[21-24] One idea is that supporting proteins dedicate the fate of the given helicase to a specific process, this thought is supported by the finding that Mms1 supports the binding of Pif1 to a set of G4 motifs located on the lagging strand template of DNA replication.[26]

The yeast Mgs1 (Maintenance of genome stability 1) protein belongs to a highly conserved AAA^+ ATPase family[42] and it is homologous to the *Escherichia coli* RarA (also known as MgsA)[43] and human WRNIP1 (Werner Interacting Protein 1).[44] Mgs1, as well as its human homolog, plays a crucial role in genome maintenance.[42,44] Cells lacking Mgs1 show an elevated rate of mitotic recombination and Mgs1 overexpression sensitizes cells to DNA damaging agents, such as MMS, HU, and UV-light.[42,45,46] Despite the various published phenotypes related to nonphysiological levels of Mgs1[45,46] the exact function of Mgs1 is not clear. However, based on previous findings Mgs1 has multiple roles in the preservation of genomic integrity.[42,45-51] Mgs1 has been shown (i) to function in a special pathway of post-replicative DNA repair,[45,46,48,52] (ii) to contribute to the maintenance of proper DNA topology,[42,47] and (iii) to Okazaki fragment maturation.[49] Moreover, Mgs1 interacts with DNA polymerase δ, leading to the postulation of two additional models. In the first model, Mgs1 supports the removal of DNA polymerase δ from the replication fork by physically interfering with the ubiquitylated PCNA-DNA polymerase δ interaction.[48,50] In the second model, Mgs1 becomes indispensable for cell survival through a currently unknown biochemical mechanism in which both the Rad6-dependent DNA damage tolerance and homologous recombination pathways are blocked.[46] It is also known that the function of Mgs1 and WRNIP1 is linked to RecQ helicases. This is based on the fact that WRNIP1 physically interacts with one of the human RecQ helicases, called WRN[53,54] and in yeast the *sgs1*Δ *mgs1*Δ double mutant shows a slow-growth phenotype and elevated number of recombination events.[45,47]

In this work, via combination of in vitro and in vivo analyses we demonstrate that Mgs1 is a novel G4-binding protein supporting genome stability. Biochemical analyses allowed us to identify Mgs1 as a novel binder of G4 structures. In vivo Chromatin Immunoprecipitation (ChIP) experiments confirm these in vitro observations, by showing that Mgs1 binds to G4 motifs in yeast. A combination of gross chromosomal rearrangement (GCR) assays, ChIP, and growth analysis of Mgs1 deficient cells in the presence and absence of

TABLE 1 Sequences of DNA oligonucleotides used in gel shift and fluorescence anisotropy experiments

Name	Type	Sequence (5′-3′)[a]	Label
MYC (c-Myc2345)	G4	TGA**GGGTGGGTA**GGGTGGGTGCGTCTGCGGCTGGCTCGAGGC	5′ FITC
	Control	GTGAGATGTTGACCATGGGTGCGTCTGCGGCTGGCTCGAGGC	5′ FITC or Cy3
	GC-rich control	TGAGTGTGAGTGGTGTGAGAGCGGCGGCGGCTGGCGCGAGGC	5′ FITC
	C-rich control	ACTCCCACCCATCCCACCCACGCAGACGCCGACCGAGCTCCG	5′ FITC
Complementary strand		TTTGCCTCGAGCCAGCCGCAGACG	–

Note: Guanines involved in G4 structure formation are in bold.

PhenDC$_3$, a G4-stabilizing agent, revealed that the binding of Mgs1 at G4 motifs is linked to changes in helicase expression and genome stability events.

2 | MATERIALS AND METHODS

2.1 | cDNA cloning, protein expression, and purification

The cDNA encoding full-length yeast Mgs1 protein was cloned into the pENTR4 Gateway entry vector (Thermo Fischer, Waltham, MA, USA) using *Nco*I and *Eco*RI restriction enzymes (Thermo Fischer, Waltham, MA, USA), resulting in pBP298 plasmid. For Mgs1 protein expression the Mgs1 cDNA was cloned in fusion with N-terminal glutathione S-transferase (GST) tag under the control of the *S. cerevisiae* galactose-inducible phosphoglycerate promoter using the Gateway cloning system (Invitrogen, Waltham, MA, USA), which resulted in pBP309 plasmid.

The Mgs1 protein was overexpressed in the protease-deficient BJ5464 yeast strain. Cells were grown to stationer phase in synthetic medium lacking leucine to select for the plasmids. The cultures were diluted 10-fold in fresh medium lacking dextrose, but containing 2% of lactic acid and 3% of glycerol. This was followed by overnight incubation with addition of galactose to 0.2% of final concentration. Cells were harvested and disrupted after a 10-hour incubation at 30°C in buffer P (20 mM Tris-HCl pH 7.5, 1 mM dithiothreitol (DTT), 0.01% v/v Nonidet P-40, 10% v/v glycerol) supplemented with 1 M of NaCl, 5 mM of EDTA, and protease inhibitor mixture (Roche Applied Science, Basel, Switzerland). After centrifugation, the supernatant of the cell extract was loaded onto glutathione-Sepharose (GE healthcare, Chicago, IL, USA) columns. First, the column was washed with buffer P + 1 M NaCl followed by washing with buffer P + 500 mM KCl. The GST-Mgs1 protein was eluted with 20 mM of reduced glutathione in buffer P supplemented with 500 mM of KCl. Mgs1-containing fractions were concentrated with Microcon-30 (Merck Millipore, Burlington, MA, USA), frozen in liquid nitrogen, and stored at −80°C.

2.2 | Preparation of DNA molecules

DNA sequences of the oligonucleotides used for gel shift and fluorescence anisotropy experiments are listed in Table 1. DNA substrates were prepared by heating of the applicable oligonucleotides (500 nM concentration) at 95°C for 5 minutes and cooling overnight to room temperature in buffer A (25 mM Tris-HCl pH 7.5, 50 mM KCl). All DNA substrates were stored at 4°C.

2.3 | Gel shift assays

Different concentrations of purified GST-Mgs1 (as indicated in the figures) were incubated with 50 nM of fluorescein- and/or Cy3-labeled DNA substrates in buffer R (25 mM Tris-HCl pH 7.5, 150 mM KCl, 1 mM DTT, 20 ng/μL BSA) for 15 minutes at 25°C. In the experiments testing the ATP and Mg^{2+} dependence of the interaction buffer R was supplemented with 1 mM of ATP and 5 mM of $MgCl_2$. Samples were run on a 4% native polyacrylamide gel in 0.5 X TB (45 mM Tris-borate) buffer, and imaged using a Typhoon Trio Imager (GE Healthcare, Chicago, IL, USA). The binding efficiency was calculated from band intensities from the shown picture measured using ImageJ software.

2.4 | Fluorescence anisotropy measurements

Measurements were carried out in buffer B (50 mM Tris-HCl pH 7.5, 90 mM KCl, 5 mM EDTA). 5′ fluorescein labeled DNA molecules at 10 nM concentration were titrated with increasing concentrations of Mgs1 at 25°C. Fluorescence anisotropy was measured in a Synergy H4 Hybrid Multimode microplate reader (BioTek, Winooski, VE, USA).

2.5 | ATPase assay

Steady-state ATPase experiments were carried out in buffer C (50 mM Tris-HCl pH 7.5, 50 mM KCl, 50 mM NaCl, 5 mM $MgCl_2$, 50 μg/mL BSA) by using a pyruvate

kinase-lactate dehydrogenase (PK-LDH) coupled assay (14 U/mL PK, 20 U/mL LDH, 1 mM ATP (Roche Applied Science, Basel, Switzerland), 1 mM phosphoenol pyruvate, 200 μM NADH) at 25°C. Time courses of NADH absorbance ($\varepsilon_{340} = 6220\ M^{-1}\ cm^{-1}$) were followed in an Infinite F Nano+ microplate reader (Tecan, Männedor, Switzerland).

2.6 | Data analysis

Means ± SEM values are reported in the paper, unless otherwise specified. Sample sizes (n) are given for the number of ensemble in vitro measurements performed using independent protein preparations (biological replicates, $n = 3$ unless otherwise specified). Data analysis was performed using Origin 8.0 (OriginLab corp).

2.7 | Strains, constructs, and media

All yeast strains used are listed in Table 2. All experimental strains are derivatives of the RAD5+ version of W303 (a gift from R. Rothstein) or the YPH background. Deletion strains harboring eliminated entire ORFs were created as published previously.[55] Epitope tagging to generate Mgs1-Myc13 was carried out as described previously.[56] The mutation of the G4 motif on Chromosome VI was created using the Cre-LoxP system as previously described.[26]

2.8 | Gross chromosomal rearrangement (GCR) assay

The GCR assay was performed as previously described[57] with minor modifications. Briefly, per strain seven different colonies were grown for 48 hours. After washing, cells were plated in different dilutions on two plates: One reference plate (rich media YPD) and one selective FOA/CAN plate. On the reference plate, all cells will grow, on the selective plate only those will grow which lost, by an GCR event, both counter-selectable markers. Colony formation on both plates was used to determine the GCR rate via fluctuation analysis using FALCOR and the MSS maximum likelihood method.[58]

TABLE 2 List of yeast strains used in this study

Strain	Genotype	Source
W303	*MATa ura3-1 trp1-1 leu2-3,112 his3-11,15 ade2-1 can1-100 ybp1-1 RAD5+*	R. Rothstein
MBY49	*MATα ura3-52 lys2-801_amber ade2-101_ochre trp1Δ63 his3Δ200 leu2Δ1 hxt13::URA3*	[22]
SG64	*MATα ura3-52 lys2-801_amber ade2-101_ochre trp1Δ63 his3Δ200 leu2Δ1 hxt13::URA3 prb1::*G4(ChrI)- *LEU2*	[22]
QL12	*MATα ura3-52 lys2-801_amber ade2-101_ochre trp1Δ63 his3Δ200 leu2Δ1 hxt13::URA3 mgs1::TRP1*	This study
QL2, QL17, QL21, QL22, QL23	*MATα ura3-52 lys2-801_amber ade2-101_ochre trp1Δ63 his3Δ200 leu2Δ1 hxt13::URA3 prb1::*G4(ChrI)- *LEU2 mgs1::TRP1*	This study
QL0	W303 *mgs1Δ::TRP1*	This study
KW200	*MATα ura3-52 lys2-801_amber ade2-101_ochre trp1Δ63 his3Δ200 leu2Δ1 hxt13::URA3 prb1::*NG(ChrVIII)- *LEU2*	[26]
KW203	*MATα ura3-52 lys2-801_amber ade2-101_ochre trp1Δ63 his3Δ200 leu2Δ1 hxt13::URA3 prb1::*GR(ChrI)- *LEU2*	[26]
QL15	*MATα ura3-52 lys2-801_amber ade2-101_ochre trp1Δ63 his3Δ200 leu2Δ1 hxt13::URA3 prb1::*NG(ChrVIII)- *LEU2 mgs1::TRP1*	This study
QL16	*MATα ura3-52 lys2-801_amber ade2-101_ochre trp1Δ63 his3Δ200 leu2Δ1 hxt13::URA3 prb1::*GR(ChrI)- *LEU2 mgs1::TRP1*	This study
QL24, QL25, QL26	W303 Mgs1-Myc13*::TRP1*	This study
TZ25	W303 Mgs1-Myc13*::TRP1, G4 Chr IV mut-LoxP*	This study

TABLE 3 Primer sequences for qPCR analysis after ChIP

qPCR Primer	Location	primer	G4 motif of interest near qPCR primer
KW75/76	Chr IV, control	CGAAGTATACCGTGCGTC	
		AGCTTCTTGCTGCTCTATG	
KW 77/78	Chr XIII, control	GAGGACGAAACGATTGATG	
		AGATAATGAGCCACGGTAC	
KW 73/74	Chr I, control	TTCCACGTAGCAGTCCTC	
		GAGGCCTCCGGAATTTTG	
KW 70/71	Chr V, control	AAATCCCACCACATCCATC	
		AACGTATACGTCGATGATAC	
TZ22	Chr IV,	GAACGTCAATATGTAGCGG	
		GACTTAGGATGACTGATGG	**GG**AT**GG**AA**GGG**TTGTAGCT**GG**
KW61/KW62	Chr VI G4, G4 mut	TGCATAGTTCTTAGGTCTTC	**GGGG**CACACGTGC**GGG**AGTTTCAAA**GGGG** CAGAATAGT**GGGG**TTCA**GGGG**
		GTATAGCAGTGACGCGTG	GGCGCACACGTGCGCGAGTTTCAAAGGCG CAGAATAGTGCGCTTCAGCCG)
KW278/KW279	Chr XI, G4	ACTAGGTCTCTTAGCTCTC	**GGG**AACT**GG**TCTCTT**GGG**CTAAAGG
		TTTTGAACACGTTCTACGAG	
KW195/KW196	ChrXIIIa, G4	GCTTCAGCCTGGGGTAAC	**GGGGCGG**CCAA**GG**TACT**GG**
		GGCACCATTAGATTCACCAC	
KW63/KW64	ChrXIIIb, G4	AAGGTAATGGAGGTGCATC	**GGGGCGG**CCAA**GG**TACT**GG**
		CTCCGCCATCTCTTGTAC	
KP 173	Chr XV, G4	CATAGTTTACCGCCTTTACC	**GGCGGAGGAGG**
		GGGAATGGAAATGGATTGC	

Note: that, here only the closest G4 motif is indicated but at most cases additional G4 motifs were mapped within the shearing range of the experiment (average fragment size 1000 bp). The G-tracts of the G4 motifs are highlighted in bold. Underlined G4 tracts were mutated in the used cre-loxP system to avoid G4 formation.

2.9 | Multiplex PCR

In brief, genomic DNA isolated from *S. cerevisiae* strains that survived the GCR events were analyzed by multiplex PCR using published primers[22] and the following cycling parameters: initial denaturation for 5 minutes at 95°C, 35 cycles of 95°C for 30 seconds, 56°C for 30 seconds, and 72°C for 45 seconds, and a final extension at 72°C for 10 minutes. PCR products (10 μL per reaction) were run at 90 V on 2.5% of agarose gels containing ethidium bromide and visualized by ultraviolet transillumination.

2.10 | Growth assay

Overnight cultures of *S. cerevisiae* cells were grown and used to inoculate to OD_{600} 0.15. After the first 90 minutes the OD_{600} was recorded every 60 minutes until OD ~1.5 was reached. The doubling time was calculated by the following formula: $\mu = (\log OD_2 - \log OD_1)/(t_2 - t_1)$; $t_{\text{doubling time}} = \ln_2/\mu$. $PhenDC_3$ (10 μM final concentration, from 2 mM stock in DMSO) was added in YPD culture when inoculated. As control DMSO was used (same concentration as within $PhenDC_3$ samples = 0.5%). OD_{600} was recorded at the same time points as in the case of control strains.

2.11 | Chromatin Immunoprecipitation (ChIP)

ChIP of asynchronous yeast cells was performed as described.[23,26] Anti-Myc antibody (*Clontech* monoclonal ab #631206) was used in the experiments. qPCR analysis was performed on a Roche Biocycler using the amount of DNA in ChIP and input for quantification. qPCR primers are listed in Table 3. The ChIP experiment was repeated for at least three biological replicates at each locus. In all cases the percentage signal (IP) was normalized to the amount of input and compared to values (IP/input) of wild-type samples.

2.12 | Yeast one-hybrid screen

The yeast one-hybrid screen was performed as previously described[59] using the Matchmaker Gold Yeast One-Hybrid Library Screening (*Clontech*, Kyoto, Japan). Briefly, a G4

motif from chromosome IX ($G4_{IX}$) was cloned into the *S. cerevisiae* Y1HGold genome as described in the manual. As a control bait, a mutated G4 motif (mut-$G4_{IX}$,) was cloned using the same method. The minimal inhibitory concentration of aureobasidin A (AbA) was determined and screen was performed using yeast cDNA library (DUAL hybrid cDNA library). Positive hits were re-striked on selective plates and plasmids of library were isolated, cloned, and sequenced.

3 | RESULTS

3.1 | Mgs1 is a G-quadruplex DNA-binding protein

In a yeast one-hybrid screen (manuscript in preparation) using a G4 motif as bait, we identified, among others,[26,59] Mgs1 as a potential novel G4-binding protein. Mgs1 did not interact with the control bait (a mutated G4 motif, that cannot form G4 structure). Based on this screening hit, we purified Mgs1 protein from yeast with an N-terminal GST-tag (Figure 1A). To confirm G4 DNA binding by Mgs1, we performed gel shift assays using a 5′-fluorescein-labeled ssDNA molecule comprising the so-called Myc2345[60] intramolecular G4 motif of the c-MYC promoter (Table 1). Based on previous findings, the c-MYC DNA sequence forms a stable G4 structure in the presence of KCl.[60] In our substrate the G4 structure is formed at the 5′ end, which is followed by a 3′ ssDNA region 21 nt. Throughout this manuscript we will refer to this molecule as MYC ssG4. The purified Mgs1 protein was incubated with MYC ssG4 or with a control ssDNA molecule in which the G4-forming guanine bases of the Myc2345 region were replaced with other nucleobases to prevent the formation of G4 structure[60] (Table 1). In both cases the formation of DNA-protein complexes was observed (Figure 1B). In the case of the G4 DNA sample, DNA-protein complexes appeared at lower Mgs1 concentrations than in the control DNA sample (Figure 1B). These results indicate a stronger binding to the G4 structure than to the control ssDNA by Mgs1.

Several studies demonstrated that Mgs1 is part of the replication and replication fork-coupled repair machineries.[45,46,48,51] Therefore, we tested its binding affinity to partial duplex DNA substrates containing either the Myc2345 G4-forming sequence (MYC dupG4) or a non-G4-forming control sequence. Substrates were generated by annealing an oligonucleotide complementary to the 3′ ssDNA region of MYC ssG4 or to the control ssDNA molecule (Table 1). Ultimately, these structures mimic the primer-template junction of a stalled replication fork in the presence or absence of an intramolecular G4 structure. In agreement with ssDNA experiments, we observed preferential binding to the G4-containing DNA structures by Mgs1 (Figure 1C).

To verify specific G4 binding, we also carried out competition gel shift assays in which the 5′-fluorescein-labeled MYC ssG4 (Figure 1D) or MYC dupG4 molecules (Figure 1E) and 5′-Cy3-labeled versions of the control DNA molecules were both present in the same reaction in equimolar amounts. As expected, Mgs1 showed higher binding affinity to the G4-containing substrates even in the presence of the control substrate. These data further support the finding that Mgs1 specifically binds to G4 structures in vitro.

In addition to gel shift experiments, we precisely determined the dissociation constants (K_d) of Mgs1 for G4 binding in fluorescence anisotropy titration experiments (Figure 2A,B, and Table 4). In agreement with the gel shift experiments, we observed preferential binding to G4-forming substrates. Whereas previously published data about the WRNIP1, the human homologue of Mgs1, indicated multimerization of WRNIP1,[61] our obtained binding curves of Mgs1-DNA interaction were sufficiently described by a simple hyperbolic equation. Thus, we observed no signs of cooperativity in DNA binding in anisotropy experiments. Binding to MYC ssG4 ($K_d = 7 \pm 2$ nM) and dupG4 ($K_d = 24 \pm 4$ nM) was determined to be relatively strong, whereas in the case of control ssDNA ($K_d = 68 \pm 7$ nM) and partial duplex DNA molecules ($K_d = 72 \pm 15$ nM), that is, in the absence of the G4 structure, the affinity decreased by ~10 and ~3 times, respectively (Figure 2A,B and Table 4). Statistical analysis (Student's *t* test) showed a significant difference in Mgs1-DNA binding between G4 and all control substrates, both in single-stranded (P value $< .001$, control compared to G4) and partial duplex (P value $< .05$; control compared to G4) form.

To test whether Mgs1 distinguishes between guanine-rich (GC-rich) and G4-forming DNA strands, we tested the binding to other control oligonucleotides which GC-content is equal to the MYC ssG4. Besides the GC-rich control, binding to the complementary strand of the MYC ssG4 was also tested, this cytosine-rich strand conceivably might form an i-motif structure.[62,63] Binding to both the GC-rich (single-stranded: $K_d = 275 \pm 85$ nM; partial duplex: $K_d = 189 \pm 29$ nM) and the C-rich complementary strand (single-stranded $K_d = 249 \pm 33$ nM; partial duplex: $K_d = 110 \pm 20$ nM) DNA substrates was weaker compared to the G4-forming DNA substrate (Figure 2A,B and Table 4). Statistical analysis (Student's *t* test) showed a significant difference between binding affinity of G4 and all control substrates, both in single-stranded and partial duplex form (P values $< .05$ compared to G4). To further strengthen the specific G4 binding of Mgs1, we tested its binding to the G4-forming DNA substrate in the presence of Li^+ ions. It has been previously published that the formation of G4 structure is weaker in the presence of Li^+ ions.[64-67] Binding efficiency to MYC ssG4 in the presence of LiCl ($K_d = 23 \pm 4$ nM) was more than three times weaker than in

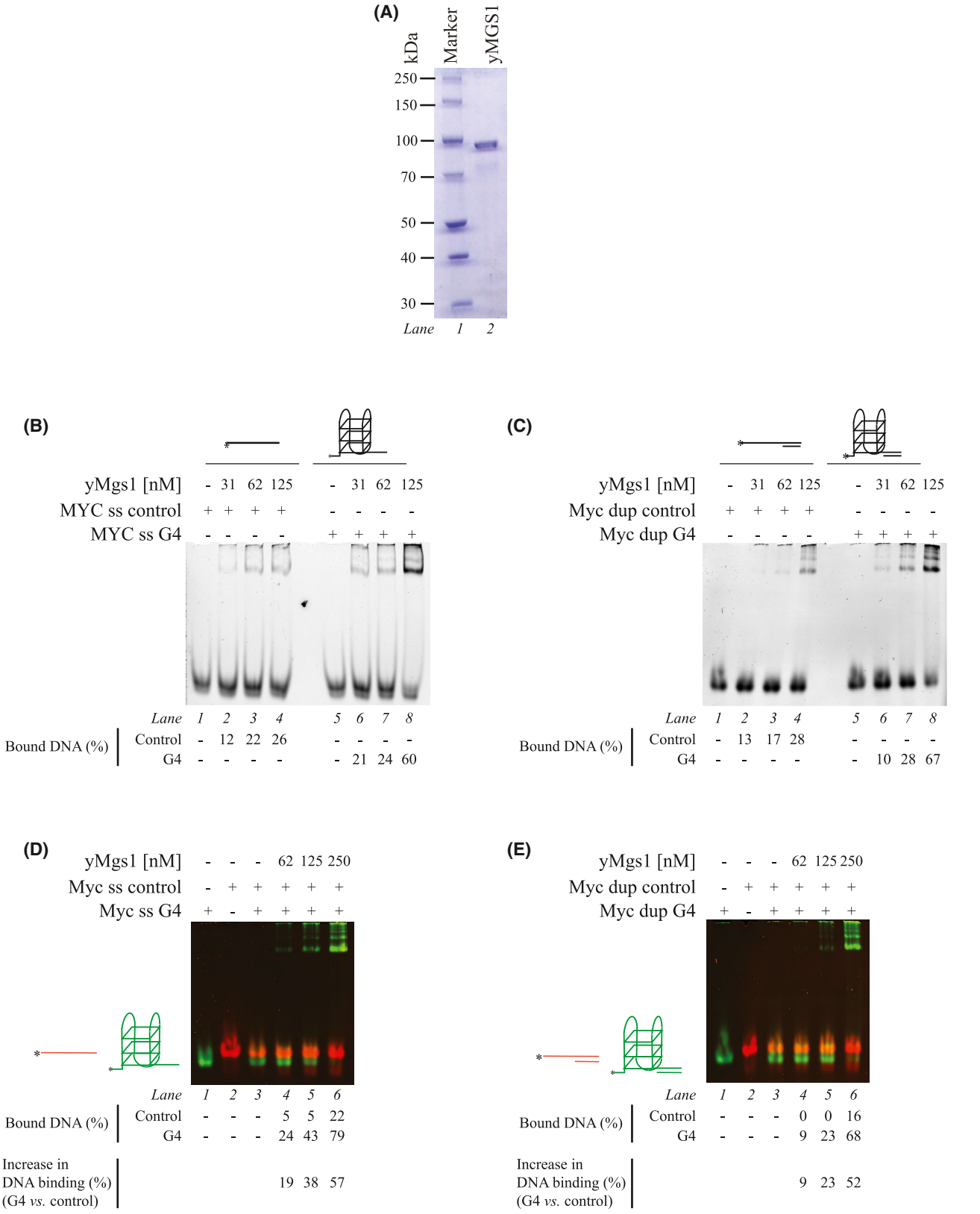

FIGURE 1 Mgs1 has robust G4-binding activity. A, Coomassie-stained SDS-PAGE (10% acrylamide) of purified yeast GST-Mgs1 protein (Mgs1 66.6 kDa; GST 26.9 kDa). B,C, Gel shift experiments carried out in the presence of (B) MYC ssG4 and control ssDNA or (C) MYC dupG4 and MYC dup control partial duplex DNA as indicated. D,E, Competitive gel shift experiment carried out in the presence of (D) FITC-labeled MYC ssG4 (green) and Cy3-labeled control ss DNA (red) or (E) FITC-labeled MYC dupG4 and Cy3-labeled MYC dup control partial duplex DNA as indicated. The samples were run on 4% of native polyacrylamide gel

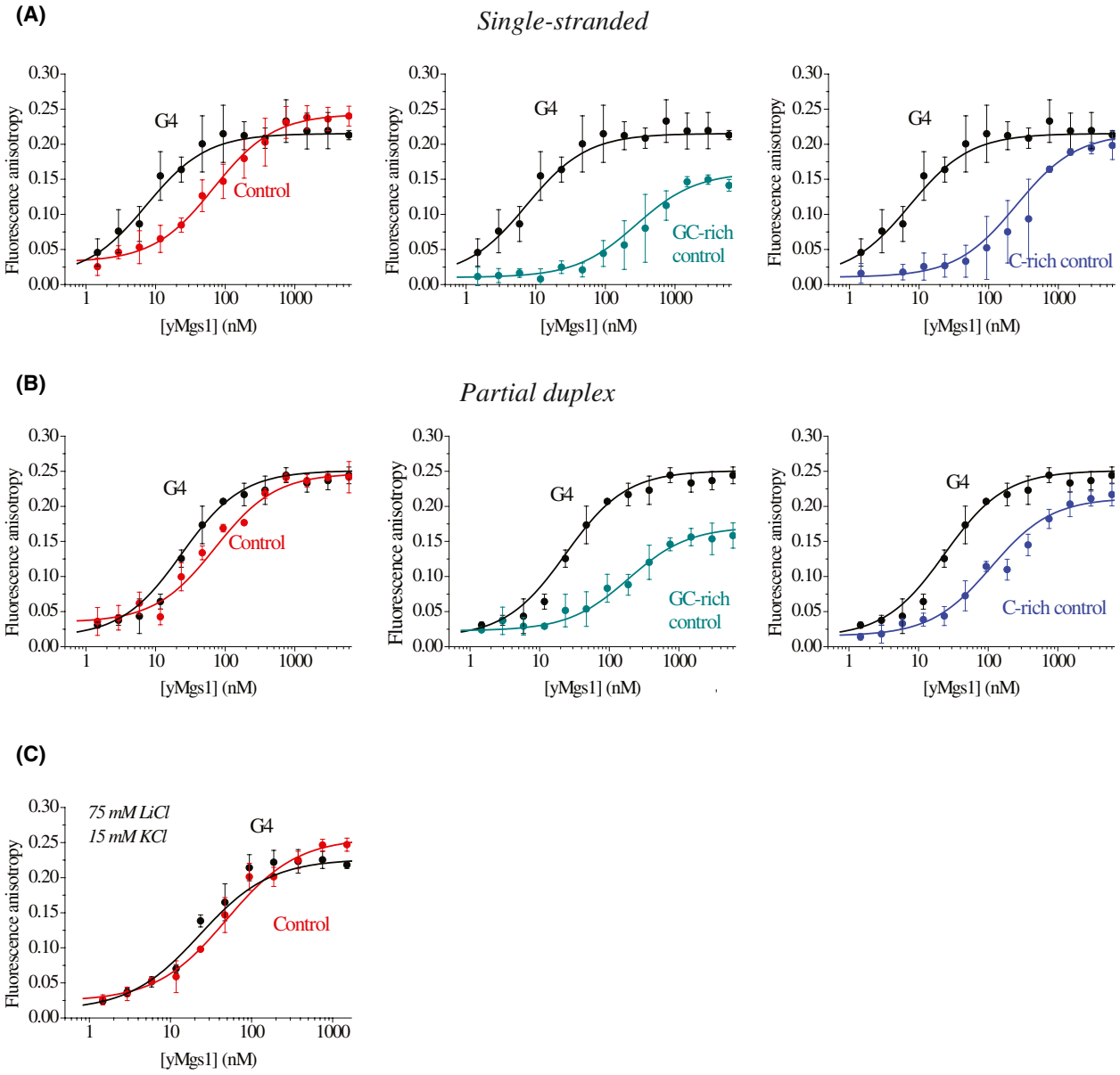

FIGURE 2 Mgs1 specifically binds to G4 structures in vitro. Results of fluorescence anisotropy titration experiments using A, single-stranded and B, partial duplex MYC G4 (black), control (red), GC-rich control (green), and C-rich (blue) DNA molecules. Solid lines are best fits to a hyperbolic binding equation, for which the Hill cooperative binding equation was used as the simple hyperbolic binding model was insufficient to describe the observed sigmoidal shape of the binding curve. Error bars represent fitting error ($n = 3$, unless otherwise specified). Significances were calculated based on the Student's t test. (A) P value compared to G4: control P value $< .001$; P values GC-control and C-rich control $p < .05$. (B) P value compared to G4: control, GC-control, and C-rich control P values $< .05$. C, Results of fluorescence anisotropy titration experiments using MYC ssG4 (black) and control DNA molecules (red) in the presence of 75 mM LiCl and 15 mM KCl. Solid lines are best fits to a hyperbolic binding equation, for which the Hill cooperative binding equation was used as the simple hyperbolic binding model was insufficient to describe the observed sigmoidal shape of the binding curve. Error bars represent fitting error (n = 3). Significance was calculated based on the Student's t test, P value compared to G4: control P value $< .05$

the presence of K^+ ions, whereas in the case of control ssDNA ($K_d = 49 \pm 4$ nM) the binding strength was similar than in the KCl buffer (Figure 2C and Table 5). We have to note here, that the protein was purified in KCl-containing buffer, therefore, in these experiments besides 75 mM LiCl 15 mM KCl was also present in the reaction buffer. DNA substrates for these experiments were prepared in LiCl-containing buffer.

3.2 | The Mgs1-G4 interaction is ATP-independent and does not alter the ATPase activity of Mgs1

Previous studies showed that Mgs1 has an inherently low ATPase activity which is slightly stimulated by single-stranded, double-stranded, or partial dsDNA.[42] Thus, it is

TABLE 4 Determined K_d values [nM] from Figure 2A,B

DNA-type		$K_d \pm$ fitting error [nM]	Biological replicates	*P* value (compared to G4)
myc Single-stranded	G4	7 ± 2	4	
	Control	68 ± 7	5	<.001
	GC-rich control	275 ± 85	3	<.05
	C-rich control	249 ± 33	3	<.05
myc Partial duplex	G4	24 ± 4	3	
	Control	72 ± 15	3	<.05
	GC-rich control	189 ± 29	3	<.05
	C-rich control	110 ± 20	3	<.05

TABLE 5 Determined K_d values [nM] from Figure 2C

DNA-type		$K_d \pm$ fitting error [nM]	Biological replicates	*P* value (compared to G4)
myc Single-stranded	G4	23 ± 4	3	
	Control	49 ± 4	3	<.05

in principle possible that different nucleotide-bound states of Mgs1 have altered binding properties to the G4 structure. However, we did not observe any difference in gel shift experiments monitoring binding of Mgs1 to the MYC ssG4 and dupG4 in the absence or presence of 1 mM ATP and 5 mM $MgCl_2$ (Supplementary Figure 1A,B) indicating that DNA binding is not influenced by Mgs1 ATPase activity. In order to precisely quantify how the presence of a G4 structure influences the ATPase rate we used a NADH-coupled ATPase assay.[68] In agreement with previous findings, the ATPase activity of Mgs1 was found to be relatively slow (4.07 ± 1.83 min^{-1}). Addition of saturating amounts (0.5 μM) of control ssDNA or MYC ssG4 stimulated the ATPase activity by 1.5 ± 0.4 and 1.6 ± 0.4 times, respectively (Supplementary Figure 1C and Table 6). Similarly, both MYC dupG4 and the control partial duplex stimulated the ATPase activity by 2.4 ± 0.3 and 2.2 ± 0.2 times, respectively (Supplementary Figure 1C and Table 6). These results indicate that the presence of the G4 structure does not influence ATPase activity. Interestingly, partial duplexes increased the Mgs1 ATPase activity to a greater extent than did ssDNA (Table 6), however, based on Student's *t* test analysis, the values did not differ in a statistically significant manner ($p = 0.82$). Nevertheless, it must be noted that even the DNA-stimulated ATPase activity of Mgs1 (5.29 ± 2.03 min^{-1} and 6.27 ± 3.48 min^{-1} for ss and partial duplex DNA, respectively) is very slow compared to yeast G4-unwinding helicases as Sgs1 (~80–200 s^{-1})[69] and Pif1 (~15 s^{-1}).[70]

Taken together, the above observations indicate that Mgs1 binds to G4-containing DNA both in the absence and presence of ATP; however, the G4 structure does not alter the weak stimulatory effect of DNA on Mgs1 ATPase activity.

TABLE 6 Measured and normalized values of Mgs1 ATPase activity from Supplementary Figure 2C.

DNA-type	ATP/min	Normalized
Mgs1 alone	4.07 ± 1.83	1
MYC ss cont	5.79 ± 1.85	1.5 ± 0.4
MYC ss G4	5.29 ± 2.03	1.6 ± 0.4
MYC dup cont	7.16 ± 3.57	2.2 ± 0.2
MYC dup G4	6.27 ± 3.48	2.4 ± 0.3

3.3 | Mgs1 is associated with G4-prone regions in vivo

Several publications indicated that the function of Mgs1 is linked to DNA replication.[45,46] Additionally, it is known that G4 structures slow-down replication, affect transcription, and other polymerase-driven processes.[71] Therefore, we assessed whether Mgs1 is related to replication fork progression at G4 motifs. To test this, we analyzed the growth of yeast cells in which we deleted *MGS1* (*mgs1*Δ). In this experiment the doubling time was experimentally determined for wild-type and *mgs1*Δ strains (90.8 ± 1.1 and 98.0 ± 1.8 minutes, respectively). This result revealed that Mgs1 deletion alone did not change the growth significantly (Figure 3A). However, if cells are treated with a G4-stabilizing ligand ($PhenDC_3$),[72] *mgs1*Δ cells grew slower (114.5 ± 4.0 minutes) compared to treated wild-type cells (91.6 ± 2.1 minuutes), indicating that Mgs1 is necessary for proper cell growth when G4 structures are stabilized by $PhenDC_3$ in vivo. We note that, $PhenDC_3$ was dissolved in DMSO to ensure that the obtained growth defect is not due to DMSO addition, as a control wild-type and *mgs1*Δ were treated with DMSO alone. These control

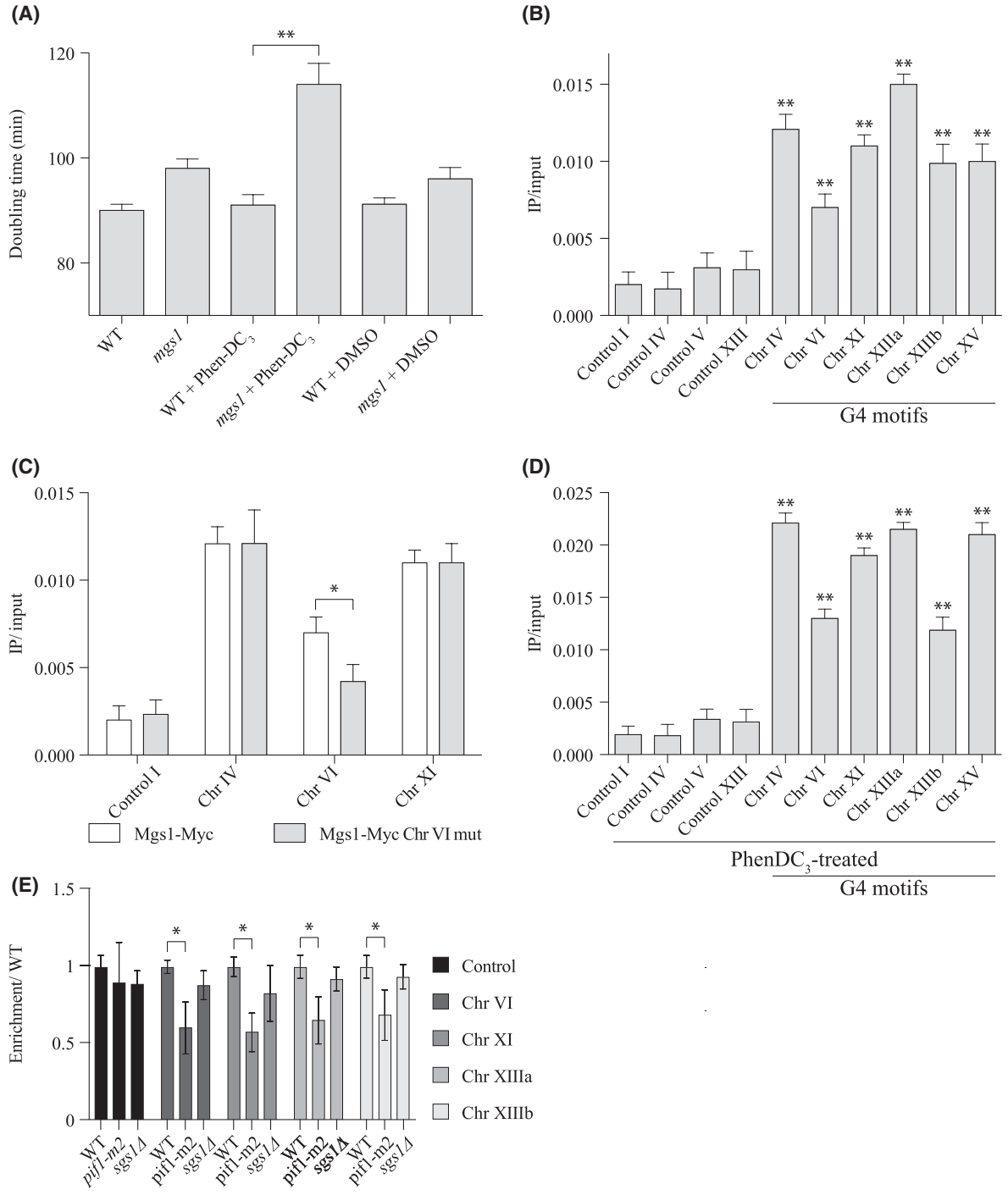

FIGURE 3 Mgs1 binds to G4 DNA structures in vivo. A, Growth analysis of *S. cerevisiae* wild-type cells (WT) and cells lacking Mgs1 (*mgs1*Δ) in the presence or absence of the G4-stabilizing ligand PhenDC$_3$. Due to the fact that PhenDC$_3$ is resolved in DMSO cells were treated with the same concentration of DMSO (0.5%). All growth analyses were performed using three biological triplicates. Significances were calculated based on the Student's *t* test (**P values < .001). B-D, Mgs1 binding to different control regions and different G4 motifs located at different yeast chromosomes (Control I, Control IV, Control V, Control XIII; Chr IV, Chr VI, Chr XI, Chr XIIIa, Chr XIIIb, Chr XV). Tested chromosome is indicated by Roman number. B, Mgs1 binding to selected regions in asynchronous growing cells. All G4 regions are significantly enriched (**P values < .001) compared to the controls. C, Mgs1 binding to different regions in the yeast genome, in this background the G4 motif from Chromosome VI was mutated in such manner that it lost the ability to form G4 structures. Similarly, to previous experiments Mgs1 binds to the G4 from Chromosome IV and XI but less to the mutated one from chromosome VI. Statistical analysis using the Student's *t* test between Chr VI G4 and Chr VI mut revealed a *P value < .01) D, Mgs1 binding in the presence of PhenDC$_3$. In all Mgs1-Myc ChIP experiments data were determined after ChIP and qPCR and normalized to input DNA. E, Mgs1 binding in wild-type, *pif1-m2*, and *sgs1*Δ yeast strains. Binding was normalized to the binding of Mgs1 in the wild-type yeast cells. For all ChIP experiments significances were calculated based on the Student's *t* test (**P values < .001 * P value < .01). All presented data are plotted as the mean plus or minus one standard deviation of three biological replicates

experiments did not show significant changes in growth compared to untreated cells (91.2 ± 1.2 and 95.0 ± 2.2 minutes, respectively).

Our in vitro findings lead to the speculation that Mgs1 can bind directly to G4 and that this effect could be direct. To test whether Mgs1 also binds to G4 motifs in vivo, binding to six selected G4 motifs and to four control regions (as indicated in Figure 3B) were analyzed by ChIP. G4 motifs have been previously identified by computational analysis or in different ChIP experiments.[9,23,26] For the ChIP experiment, Mgs1 was endogenously tagged at the C-terminus with Myc13. Asynchronously growing log-phase cultures expressing Myc-tagged Mgs1 were processed for ChIP followed by quantitative real-time PCR (qPCR) (Table 3). As controls, regions that were unable to form G4 structures as predicted by previous in silico analysis and experimental publications,[23,26] were chosen. As anticipated from the in vitro data, we observed strong binding to all six G4 motif-containing regions (Figure 3B) and weak binding to the controls. Comparing the extent of Mgs1 binding, we observed a 2.3-7.5-fold increase in the binding of Mgs1 at G4 motifs over the control regions (Table 7). To further strengthen the conclusion that Mgs1 binds to G4 motifs in vivo, we mutated a G4 motif on Chromosome VI (GGGGCACACGTGCGGG AGTTTCAAAGGGGCAGAATAGTGGGGTTCAGGGG to GG**C**GCACACGTGCG**C**GAGTTTCAAAGG**C**GCAGAAT AGTG**C**G**C**TTCAG**CC**G) using the Cre-loxP system. Mgs1 binding to this region was measured after ChIP and analyzed by qPCR. These data revealed that Mgs1 binding to the mutated G4 is twofold reduced (Figure 3C, Chr VImut), in comparison to the unaffected G4 motif on Chr IV and XI in the same strain background (Figure 3C and Table 8). Also, the binding was significantly lower in comparison to the original G4 on Chr VI (Figure 3B,C, column Chr VI). Before, we observed that cells lacking Mgs1 showed a growth defect in the presence of $PhenDC_3$. To get a more direct answer if Mgs1 is acting at stabilized G4s after $PhenDC_3$ treatment, we monitored Mgs1 binding to G4 motifs after $PhenDC_3$ treatment. At all six G4 motifs more Mgs1 binding could be detected, whereas no changes were observed at the controls (Figure 3D and Table 9). In summary, the qPCR results indicate that Mgs1 preferentially binds to G4 motifs in vivo.

In yeast the G4-unwinding helicases, Pif1 and Sgs1 have also been implicated to support DNA replication and other events that promote genome stability.[22,23,73-80] So far, the human homolog of Mgs1, called WRNIP1 has been shown to interact with the WRN RecQ helicase.[53,54] But so far, no evidence of genetic interaction between Mgs1 and Pif1 has been published. We tested if Mgs1 binding to G4 is influenced by Pif1 or Sgs1. For this experiment, we created Myc-tagged Mgs1 strains in which either *SGS1* is deleted, or *PIF1* is mutated in such a way that only the mitochondrial isoform is expressed (*pif1-m2*).[81] ChIP and qPCR analysis of these strains revealed that Mgs1 binding is significantly reduced in *pif1-m2* strains compared to Mgs1 binding in wild-type (Figure 3E). Binding of Mgs1 in *sgs1*Δ cells shown no significant changes compared to the wild-type (Figure 3E). These results indicate that the presence of Pif1 supports Mgs1 binding, whereas Sgs1 binding has no impact on Mgs1 binding to selected G4 regions.

In summary, the growth defect in cells lacking Mgs1 after $PhenDC_3$ treatment and the reduced binding of Mgs1 to G4 motifs in *PIF1* mutant cells, further strengthen the argument that Mgs1 binds and functions at G4-prone regions in vivo.

TABLE 7 Determined IP/input values from Figure 3B

qPCR region	IP/input	STEDV	Biological replicates
Control I	0.0020	0.0008	3
Control IV	0.0017	0.0011	3
Control V	0.0030	0.0009	3
Control XIII	0.0029	0.0012	3
Chr IV	0.0121	0.0009	3
Chr VI	0.0078	0.0008	3
Chr XI	0.0111	0.0007	3
Chr XIIIa	0.0151	0.0006	3
Chr XIIIb	0.0099	0.0012	3
Chr XV	0.0099	0.0011	3

TABLE 8 Determined IP/input values from Figure 3C mutated strains

qPCR region	IP/input	STEDV	Biological replicates
Control I	0.0022	0.0008	3
Chr VI mut	0.0042	0.001	3
Chr IV	0.0101	0.002	3
Chr XI	0.011	0.001	3

Note: See Table 7. for the values for the original strain.

TABLE 9 Determined IP/input values from Figure 3D

qPCR region	IP/input	STEDV	Biological replicates
Control I	0.0019	0.0007	3
Control IV	0.0018	0.0011	3
Control V	0.0034	0.0011	3
Control XIII	0.0031	0.0012	3
Chr IV	0.022	0.0011	3
Chr VI	0.013	0.0008	3
Chr XI	0.019	0.0006	3
Chr XIIIa	0.021	0.0005	3
Chr XIIIb	0.012	0.0016	3
Chr XV	0.021	0.002	3

TABLE 10 Sequences of GCR insert

GCR strain	Insert
G4 (Chr I)	**GGGGTGGGG**TGTTACTGATGAGAATT**GGGGG**AATTTTGAGATAATTGTT**GGG**
G4 ($ChrI_{mut}$)	CGCGTGCGCTGTTACTGATGAGAATTGGCGGAATTTTGAGATAATTGTTGGG
G-rich (Chr I)	ATGGTGGTCATCTCAGTAGATGTAGAGGTGAAAGTACCGGTCCATGGCTCGGT
Non-G-rich (Chr VII)	CTAATCTTTCAGCGTTGTAAATGTTGGTACCCAAACCCAATTGTCTACAAGTTTCCTTAGC

The G-tracts of the G4 motifs are highlighted in bold. Underlined G4 tracts are mutated to avoid G4 formation in the assay. See [22], for more information on strains.

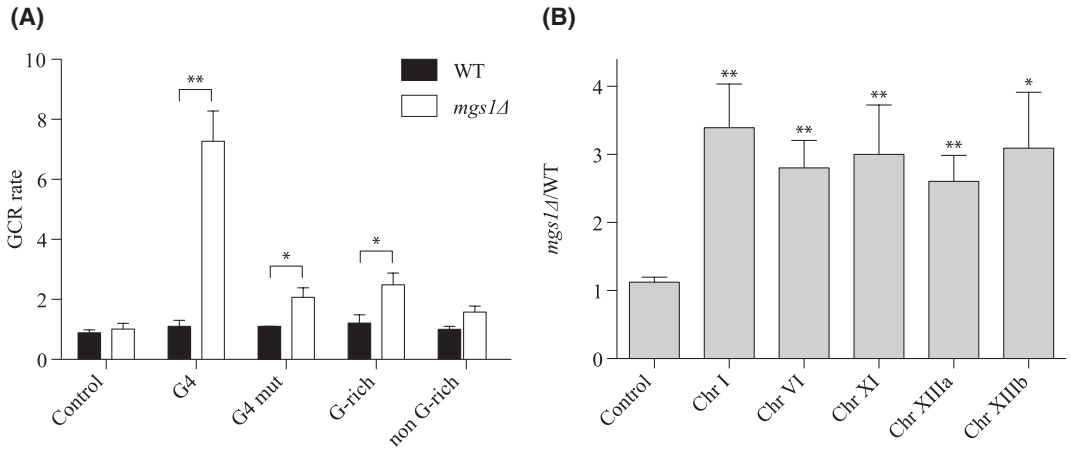

FIGURE 4 Mgs1 has an important function in the stability of G4-prone DNA regions. A, GCR analysis of wild-type (black) and *mgs1*Δ (white) strains with different inserts (no insert, G4-forming, G-rich, non-G-rich, and G4 mutated). Cells lacking Mgs1 have slightly higher GCR rate than WT. The wild-type rate of GCR events is approximately 1×10^{-10} events per generation. Statistical analysis using Student's *t* test compared to WT determined a *P* value below 0.01 using the G-rich and mutated insert (**P* value < .01), but very low *P* values (***P* value < .005) with the G4 motif as an insert. B, ChIP of γH2Ax at five different G4 motifs and a control region. ChIP was performed in wild-type and *mgs1*Δ cells. After immunoprecipitation, the associated DNA (IP), was normalized to input DNA (IP/input) and plotted. ChIP was performed in three biological replicates. IP/input values in *mgs1*Δ cells were normalized to IP/input of wild-type cells. The difference between four (except XIIIb) tested G4 regions compared to the control was significant based on the two-tailed Student's *t* test (***P* values < .001).

3.4 | Mgs1 deletion results in elevated number of genome rearrangements at G4 sites

It has been shown that deletion of *MGS1* results in elevated number of genome rearrangements.[42,45] To test if the addition of G4-prone regions affects genome instability in *mgs1*Δ cells, we performed a genetic assay that measures GCRs. GCRs, including deletions, inversions, and translocations arise by many different mechanisms.[82] Using a previously published GCR assay,[22] we quantitatively analyzed G4-dependent genome instability in the absence of *MGS1* and compared this to the GCR events of control regions. In this assay the GCR rate was measured by the simultaneous loss of two counter-selectable markers (*URA3*, *CAN1*), which are located downstream of the nonessential *PRB1* locus. The GCR rate was determined via fluctuation analysis.[58] To test the effect of Mgs1 on GCR events in the presence of G4 structures, we performed GCR analysis in wild-type and *mgs1*Δ cells harboring different DNA sequence inserts. Four different inserts were used: a G4 motif from Chr I (G4-*LEU2*), a G-rich region which cannot form G4 from Chr I (GR-*LEU2*), a non-G-rich region from Chr VII (NG-*LEU2*), as well as a mutated version of the G4 motif from Chr I (G4mut-*LEU2*) (Table 10). These regions were inserted into the yeast genome on the left arm of Chr V, replacing the nonessential *PRB1* gene. The two counter-selectable markers (URA3 and CAN1) are placed downstream of the *PRB1* region. If the inserted DNA region stimulates genome instability, both markers are lost and cells will grow on the selective plate. Cell growth will be monitored on rich- and selective-plates which will be used to calculate the GCR rate via fluctuation analysis. The GCR rate in the wild-type "no insert" cells was approximately 1×10^{-10} events per generation,[22] and none of the inserts affected this rate in wild-type background (Figure 4A and Table 11). Upon *MGS1* deletion, the GCR rate did not increase significantly in the "no insert" or "non-G-rich insert" cells, but the "G-rich insert", as well as the "G4mut insert" slightly, but not significantly, elevated the number of GCR events. Importantly, the insert with a potential to fold a G4 structure increased the GCR rate sevenfold

TABLE 11 Determined GCR rates from Figure 4A

Genotype	No insert	G4 insert	G4 mutated	G-rich insert	Non G-rich insert
Wild type	0.89 ± 0.09	1.11 ± 0.19	1.10 ± 0.004	1.21 ± 0.28	1.01 ± 0.10
mgs1Δ	1.01 ± 0.19	7.27 ± 1.01	2.07 ± 0.32	2.49 ± 0.39	1.58 ± 0.20

(Figure 4A and Table 11). PCR analysis of strains with a GCR event showed that mostly DNA deletions occurred in the absence of *MGS1* at G4 inserts (Supplementary Figure 2). From 20 colonies that grew on the GCR plates, 55% lost the fragments labeled as 1, 2, 3, and 4, 10% lost fragment 1 and 65% of the assessed colonies lost the *CAN1* gene. In the remaining 35%, all six DNA segments were still detectable. These observations indicated that Mgs1 supports genome stability at G4 motifs. Similar results were detected earlier in GCR analysis at G4 motifs in the absence Pif1 helicase.[22] To this date, we cannot state how and why these deletions occur at G4 inserts.

Based on the high frequency of deletion events observed in the GCR assay, we tested if the absence of Mgs1 resulted in an elevated amount of DNA double strand breaks (DSB). We measured the presence of phosphorylated H2A (γH2A), usually used as a regional marker for DSB [83] by ChIP and qPCR. qPCR analysis using the same primer pairs as in Figure 3B revealed that binding of γH2A is more frequent at four out of five tested G4 motifs (Chr XIIIb is not significant, due to the high standard deviation, according to Student's *t* test) compared to wild-type (Figure 4B) indicating that overall more DNA damage, likely DBSs, occurred in *mgs1*Δ cells.

4 | DISCUSSION

Genome-wide located G4 motifs show ambivalent characteristics in vivo. On the one hand, they exert important regulatory functions in basic cellular processes, such as transcription, translation, recombination, and replication.[84] On the other hand, G4 structures present obstacles for the replication machinery and, consequently, they can cause replication fork stalling and might induce DNA breaks and consequently induce genome instability.[20,21,23-25] The mechanism of replication through G4 structures is not clear yet, although the number of known G4-unwinding helicases is increasing. Both 3′-5′ and 5′-3′ helicases are potentially involved in the replication of G4 motifs, as suggested by their ability to unwind G4 structures in vitro. 5′-3′ helicases, such as Pif1 in yeast and FANCJ in human, were found as potent G4 structure-unwinding helicases.[19] Human WRN and BLM proteins (3-5′ directionality) were also shown to be able to unwind G4 structures.[32] How these helicases gain their specificity for targets and processes is not understood. It is known that proteins support helicase function such as the human WRNIP1 protein, a homologue of yeast Mgs1 that interacts with WRN helicase.[53,54] How WRNIP supports the function of WRN helicase is not clear yet. So far, this interaction has not been studied in the light of G4 unwinding.

In this study, we have described the G4 DNA binding activity of Mgs1. The interaction was identified in a genome-wide yeast one-hybrid screen and the binding in vivo was proven via ChIP and qPCR experiments in which DNA-bound Mgs1 was enriched at selected endogenous G4 motifs (Figure 3). Moreover, EMSA and fluorescence anisotropy assays supported the specific G4 binding of Mgs1 (Figures 1 and 2). Importantly, Mgs1 preferentially bound the G4-structure-containing substrates compared to the control, both in single-stranded and partial duplex form. Quantitative fluorescence anisotropy measurements showed 3- 10-fold difference in the binding affinity between the control, the GC-rich, C-rich, and G4-DNA substrates.

The finding that Mgs1 binding was significantly reduced in a *pif1-m2* background was unexpected. This finding leads to the idea that Pif1 somehow stimulates the binding of Mgs1 to the analyzed G4 sites. This phenomenon could be explained by the physical interaction between the two proteins. Unfortunately, we were not able to detect any physical interaction between Mgs1 and Pif1. Our data leads to the assumption that the recruitment of Mgs1 to the G4 sites needs the functional Pif1 helicase itself. This is underlined by the fact that in *pif1-m2* cells more G4 structures are formed and replication stalls,[23] however, less Mgs1 is bound. One speculation could be that Mgs1 supports Pif1 function at G4 regions. The cooperation mechanism between the Mgs1 and Pif1 at G4 sites is not clear yet, and needs further analysis in the near future. Although it is possible that they are cooperating either in G4 unwinding or by supporting replication restart together, or controlling/stabilizing the replication fork at G4 sites. This hypothesis is supported by GCR analysis showing that in the absence of Mgs1, similarly to Pif1 deficient cells, more GCR events were detected at G4 insert compared to control regions (Figure 4). The importance of Mgs1 at G4 sites is further strengthened by the data that in the absence of Mgs1 also high levels of γH2A occur at G4 sites, indicating that without Mgs1 more DNA damage occurs at G4 sites. Similarly, in the absence of Pif1 (also in *S. pombe*), more γH2A and DNA damage is detected at G4 sites.[23,85]

There are several observations, such as the physical interaction of Mgs1 with ubiquitylated PCNA and the synthetic lethal phenotype of *mgs1*Δ *rad18*Δ strain, which

demonstrate that Mgs1 has a tight connection to stalled replication forks.[45,46,48,50,51] Taking into consideration that human WRNIP1 interacts with DNA polymerase δ and increases its processivity and initiation frequency,[61] Mgs1 emerges as a possible candidate to assist in the replication of G4-prone DNA regions in a Pif1 dependent manner. The data presented here supports this hypothesis; cellular growth is reduced in *mgs1*Δ cells after treatment with the G4-stabilizing agent $PhenDC_3$. These data represent an additional indication that Mgs1 contributes and assists proper replication of G4 regions and that without Mgs1 G4 stabilization is a particular risk for cells (Figure 3). These growth changes are further underlined by our finding that treatment with $PhenDC_3$ results in stronger binding of Mgs1 to selected G4 regions (Figure 3D) showing the need of Mgs1 function at these stabilized G4s. Pif1 was shown to support DNA replication at G4 on the lagging strand.[74] At the lagging strand Pif1 processivity is increased by its interaction to PCNA. It could be that PCNA is the so far missing link that stimulates Mgs1 binding to Pif1 targets. Although our finding only suggest the cooperation between Mgs1 and Pif1 in the processing of G4 structures, it is possible that they might cooperate in other cellular processes as well, Okazaki fragment maturation,[49,86,87] rDNA replication,[47,88] and rescuing of the stalled replication forks,[2,45,48,50,51,73,74,87,89] as their role in these processes is already know. Further analysis of the role of these proteins in the mentioned cellular processes would be interesting.

The importance of Mgs1 for the proper maintenance and replication of G4 motifs was demonstrated in GCR assays, which showed a remarkable increase in the frequency of GCR events at G4 motifs in *mgs1*Δ cells. Contrarily, at sites containing G-rich (but not G4-prone) and control sequences, the GCR frequency was only slightly increased, which underscores the specificity of Mgs1 to G4 structures in the case of the observed GCR events (Figure 4A). The increased instability at G4-prone regions caused by the loss of Mgs1 is also corroborated by the previously published observation where the increased rDNA recombination frequency in *mgs1*Δ strain has been shown.[47] Although Mgs1 exerts a DNA-dependent ATPase activity,[42] we found that the presence of the G4 structure does not stimulate its ATPase activity to a higher extent than does the control DNA. Based on these findings, we propose structural rather than catalytic function of Mgs1 in the preservation of genomic stability at G4-prone regions.

ACKNOWLEDGMENTS

This work was supported by the Emmy-Noether Program of the Deutsche Forschungsgemeinschaft [to K.P.]; ERC Stg Grant [638988-G4DSB to K.P.]; National Natural Science Foundation of China [31700716 to Q.Y.]; National Research Development and Innovation Office [NKFIH K-119361 to P.B., NKFIH K-116072 to M.K., NKFIH K-123989 to M.K.]; ELTE KMOP [4.2.1/BOP 6072 to M.K.]; the Premium Postdoctoral Program of the Hungarian Academy of Sciences [to G.M.H.]; and Bolyai Janos Research Fellowship [to P.B.]. We thank Lajos Haracska and Lajos Pinter for the yMgs1 cDNA and plasmids. We thank Stefan Juranek and Markus Sauer for carefully reading of the manuscript. We thank K. Wanzek for inital experiments testing Mgs1 as a G4 binder.

CONFLICT OF INTEREST

None declared.

AUTHOR CONTRIBUTIONS

A. Toth, G. Harami, T. Zacheja, K. Paeschke, and P. Burkovics designed research; A. Toth, G. Harami, T. Zacheja, Q. Yang, K. Paeschke, and P. Burkovics analyzed data; A. Toth, G. Harami, T. Zacheja, Q. Yang, E. Schwindt, and P. Burkovics performed research; A. Toth, G. Harami, M. Kovacs, Q. Yang, K. Paeschke, and P. Burkovics wrote the paper.

REFERENCES

1. Aguilera A, Garcia-Muse T. Causes of genome instability. *Annu Rev Genet*. 2013;47:1-32.
2. Bochman ML, Paeschke K, Zakian VA. DNA secondary structures: stability and function of G-quadruplex structures. *Nat Rev Genet*. 2012;13:770-780.
3. Chen Y, Yang D. Sequence, stability, and structure of G-quadruplexes and their interactions with drugs. *Curr Protoc Nucleic Acid Chem* Chapter 17. 2012;Unit17 15.
4. Lipps HJ, Rhodes D. G-quadruplex structures: in vivo evidence and function. *Trends Cell Biol*. 2009;19:414-422.
5. Hansel-Hertsch R, Di Antonio M, Balasubramanian S. DNA G-quadruplexes in the human genome: detection, functions and therapeutic potential. *Nat Rev Mol Cell Biol*. 2017;18:279-284.
6. Huppert JL, Balasubramanian S. G-quadruplexes in promoters throughout the human genome. *Nucleic Acids Res*. 2007;35:406-413.
7. Marsico G, Chambers VS, Sahakyan AB, et al. Whole genome experimental maps of DNA G-quadruplexes in multiple species. *Nucleic Acids Res*. 2019;47:3862-3874.
8. Todd AK, Neidle S. Mapping the sequences of potential guanine quadruplex motifs. *Nucleic Acids Res*. 2011;39:4917-4927.
9. Capra JA, Paeschke K, Singh M, Zakian VA. G-quadruplex DNA sequences are evolutionarily conserved and associated with distinct genomic features in *Saccharomyces cerevisiae*. *PLoS Comput Biol*. 2010;6:e1000861.
10. Hershman SG, Chen Q, Lee JY, et al. Genomic distribution and functional analyses of potential G-quadruplex-forming sequences in *Saccharomyces cerevisiae*. *Nucleic Acids Res*. 2008;36:144-156.
11. Cogoi S, Xodo LE. G-quadruplex formation within the promoter of the KRAS proto-oncogene and its effect on transcription. *Nucleic Acids Res*. 2006;34:2536-2549.
12. Gray LT, Vallur AC, Eddy J, Maizels N. G quadruplexes are genomewide targets of transcriptional helicases XPB and XPD. *Nat Chem Biol*. 2014;10:313-318.
13. Moye AL, Porter KC, Cohen SB, et al. Telomeric G-quadruplexes are a substrate and site of localization for human telomerase. *Nat Commun*. 2015;6:7643.

14. Paeschke K, Juranek S, Simonsson T, Hempel A, Rhodes D, Lipps HJ. Telomerase recruitment by the telomere end binding protein-beta facilitates G-quadruplex DNA unfolding in ciliates. *Nat Struct Mol Biol*. 2008;15:598-604.
15. Paeschke K, Simonsson T, Postberg J, Rhodes D, Lipps HJ. Telomere end-binding proteins control the formation of G-quadruplex DNA structures in vivo. *Nat Struct Mol Biol*. 2005;12:847-854.
16. Siddiqui-Jain A, Grand CL, Bearss DJ, Hurley LH. Direct evidence for a G-quadruplex in a promoter region and its targeting with a small molecule to repress c-MYC transcription. *Proc Natl Acad Sci USA*. 2002;99:11593-11598.
17. Estep KN, Butler TJ, Ding J, Brosh RM Jr. G4-interacting DNA helicases and polymerases: potential therapeutic targets. *Curr Med Chem*. 2017(no.), 2881–2897.
18. Mendoza O, Bourdoncle A, Boule JB, Brosh RM Jr, Mergny JL. G-quadruplexes and helicases. *Nucleic Acids Res*. 2016;44:1989-2006.
19. Sauer M, Paeschke K. G-quadruplex unwinding helicases and their function in vivo. *Biochem Soc Trans*. 2017;45:1173-1182.
20. Castillo Bosch P, Segura-Bayona S, Koole W, et al. FANCJ promotes DNA synthesis through G-quadruplex structures. *EMBO J*. 2014;33:2521-2533.
21. Lopes J, Piazza A, Bermejo R, et al. G-quadruplex-induced instability during leading-strand replication. *EMBO J*. 2011;30:4033-4046.
22. Paeschke K, Bochman ML, Garcia PD, et al. Pif1 family helicases suppress genome instability at G-quadruplex motifs. *Nature*. 2013;497:458-462.
23. Paeschke K, Capra JA, Zakian VA. DNA replication through G-quadruplex motifs is promoted by the *Saccharomyces cerevisiae* Pif1 DNA helicase. *Cell*. 2011;145:678-691.
24. Ribeyre C, Lopes J, Boule JB, et al. The yeast Pif1 helicase prevents genomic instability caused by G-quadruplex-forming CEB1 sequences in vivo. *PLoS Genet*. 2009;5:e1000475.
25. London TB, Barber LJ, Mosedale G, et al. FANCJ is a structure-specific DNA helicase associated with the maintenance of genomic G/C tracts. *J Biol Chem*. 2008;283:36132-36139.
26. Wanzek K, Schwindt E, Capra JA, Paeschke K. Mms1 binds to G-rich regions in *Saccharomyces cerevisiae* and influences replication and genome stability. *Nucleic Acids Res*. 2017;45:7796-7806.
27. Byrd AK, Raney KD. A parallel quadruplex DNA is bound tightly but unfolded slowly by pif1 helicase. *J Biol Chem*. 2015;290:6482-6494.
28. Duan XL, Liu NN, Yang YT, et al. G-quadruplexes significantly stimulate Pif1 helicase-catalyzed duplex DNA unwinding. *J Biol Chem*. 2015;290:7722-7735.
29. Hou XM, Wu WQ, Duan XL, et al. Molecular mechanism of G-quadruplex unwinding helicase: sequential and repetitive unfolding of G-quadruplex by Pif1 helicase. *Biochem J*. 2015;466:189-199.
30. Rogers CM, Wang JC, Noguchi H, Imasaki T, Takagi Y, Bochman ML. Yeast Hrq1 shares structural and functional homology with the disease-linked human RecQ4 helicase. *Nucleic Acids Res*. 2017;45:5217-5230.
31. Sun H, Bennett RJ, Maizels N. The *Saccharomyces cerevisiae* Sgs1 helicase efficiently unwinds G-G paired DNAs. *Nucleic Acids Res*. 1999;27:1978-1984.
32. Mohaghegh P, Karow JK, Brosh RM Jr, Bohr VA, Hickson ID. The Bloom's and Werner's syndrome proteins are DNA structure-specific helicases. *Nucleic Acids Res*. 2001;29:2843-2849.
33. Wu CG, Spies M. G-quadruplex recognition and remodeling by the FANCJ helicase. *Nucleic Acids Res*. 2016;44:8742-8753.
34. Brosh RM Jr. DNA helicases involved in DNA repair and their roles in cancer. *Nat Rev Cancer*. 2013;13:542-558.
35. Croteau DL, Popuri V, Opresko PL, Bohr VA. Human RecQ helicases in DNA repair, recombination, and replication. *Annu Rev Biochem*. 2014;83:519-552.
36. Larsen NB, Hickson ID. RecQ helicases: conserved guardians of genomic integrity. *Adv Exp Med Biol*. 2013;767:161-184.
37. Suhasini AN, Brosh RM Jr. Disease-causing missense mutations in human DNA helicase disorders. *Mutat Res*. 2013;752:138-152.
38. van Wietmarschen N, Merzouk S, Halsema N, Spierings DCJ, Guryev V, Lansdorp PM. BLM helicase suppresses recombination at G-quadruplex motifs in transcribed genes. *Nat Commun*. 2018;9:271.
39. Huber MD, Lee DC, Maizels N. G4 DNA unwinding by BLM and Sgs1p: substrate specificity and substrate-specific inhibition. *Nucleic Acids Res*. 2002;30:3954-3961.
40. Smith JS, Chen Q, Yatsunyk LA, et al. Rudimentary G-quadruplex-based telomere capping in *Saccharomyces cerevisiae*. *Nat Struct Mol Biol*. 2011;18:478-485.
41. Lee JY, Mogen JL, Chavez A, Johnson FB. Sgs1 RecQ helicase inhibits survival of *Saccharomyces cerevisiae* cells lacking telomerase and homologous recombination. *J Biol Chem*. 2008;283:29847-29858.
42. Hishida T, Iwasaki H, Ohno T, Morishita T, Shinagawa H. A yeast gene, MGS1, encoding a DNA-dependent AAA(+) ATPase is required to maintain genome stability. *Proc Natl Acad Sci USA*. 2001;98:8283-8289.
43. Shibata T, Hishida T, Kubota Y, Han YW, Iwasaki H, Shinagawa H. Functional overlap between RecA and MgsA (RarA) in the rescue of stalled replication forks in *Escherichia coli*. *Genes Cells*. 2005;10:181-191.
44. Yoshimura A, Seki M, Enomoto T. The role of WRNIP1 in genome maintenance. *Cell Cycle*. 2017;16:515-521.
45. Branzei D, Seki M, Onoda F, Enomoto T. The product of *Saccharomyces cerevisiae* WHIP/MGS1, a gene related to replication factor C genes, interacts functionally with DNA polymerase delta. *Mol Genet Genomics*. 2002;268:371-386.
46. Hishida T, Ohno T, Iwasaki H, Shinagawa H. *Saccharomyces cerevisiae* MGS1 is essential in strains deficient in the RAD6-dependent DNA damage tolerance pathway. *EMBO J*. 2002;21:2019-2029.
47. Branzei D, Seki M, Onoda F, Yagi H, Kawabe Y, Enomoto T. Characterization of the slow-growth phenotype of S. cerevisiae Whip/Mgs1 Sgs1 double deletion mutants. *DNA Repair*. 2002;1:671-682.
48. Hishida T, Ohya T, Kubota Y, Kamada Y, Shinagawa H. Functional and physical interaction of yeast Mgs1 with PCNA: impact on RAD6-dependent DNA damage tolerance. *Mol Cell Biol*. 2006;26:5509-5517.
49. Kim JH, Kang YH, Kang HJ, et al. In vivo and in vitro studies of Mgs1 suggest a link between genome instability and Okazaki fragment processing. *Nucleic Acids Res*. 2005;33:6137-6150.
50. Saugar I, Parker JL, Zhao S, Ulrich HD. The genome maintenance factor Mgs1 is targeted to sites of replication stress by ubiquitylated PCNA. *Nucleic Acids Res*. 2012;40:245-257.
51. Vijeh Motlagh ND, Seki M, Branzei D, Enomoto T. Mgs1 and Rad18/Rad5/Mms2 are required for survival of *Saccharomyces cerevisiae* mutants with novel temperature/cold sensitive

alleles of the DNA polymerase delta subunit, Pol31. *DNA Repair*. 2006;5:1459-1474.

52. Barbour L, Xiao W. Regulation of alternative replication bypass pathways at stalled replication forks and its effects on genome stability: a yeast model. *Mutat Res*. 2003;532:137-155.
53. Kawabe Y, Branzei D, Hayashi T, et al. A novel protein interacts with the Werner's syndrome gene product physically and functionally. *J Biol Chem*. 2001;276:20364-20369.
54. Kawabe Y, Seki M, Yoshimura A, et al. Analyses of the interaction of WRNIP1 with Werner syndrome protein (WRN) in vitro and in the cell. *DNA Repair*. 2006;5:816-828.
55. Sikorski RS, Hieter P. A system of shuttle vectors and yeast host strains designed for efficient manipulation of DNA in *Saccharomyces cerevisiae*. *Genetics*. 1989;122:19-27.
56. Van Driessche B, Tafforeau L, Hentges P, Carr AM, Vandenhaute J. Additional vectors for PCR-based gene tagging in *Saccharomyces cerevisiae* and Schizosaccharomyces pombe using nourseothricin resistance. *Yeast*. 2005;22:1061-1068.
57. Putnam CD, Kolodner RD. Determination of gross chromosomal rearrangement rates. *Cold Spring Harb Protoc*. 2010;2010:pdb prot5492.
58. Hall BM, Ma CX, Liang P, Singh KK. Fluctuation analysis CalculatOR: a web tool for the determination of mutation rate using Luria-Delbruck fluctuation analysis. *Bioinformatics*. 2009;25:1564-1565.
59. Götz S, Pandey S, Bartsch S, Juranek S, Paeschke K. A novel G-quadruplex binding protein in yeast—Slx9. *Molecules*. 2019;24.1774.
60. Eddy S, Ketkar A, Zafar MK, Maddukuri L, Choi JY, Eoff RL. Human Rev1 polymerase disrupts G-quadruplex DNA. *Nucleic Acids Res*. 2014;42:3272-3285.
61. Tsurimoto T, Shinozaki A, Yano M, Seki M, Enomoto T. Human Werner helicase interacting protein 1 (WRNIP1) functions as a novel modulator for DNA polymerase delta. *Genes Cells*. 2005;10:13-22.
62. Day HA, Pavlou P, Waller ZA. i-Motif DNA: structure, stability and targeting with ligands. *Bioorg Med Chem*. 2014;22:4407-4418.
63. Zeraati M, Langley DB, Schofield P, et al. I-motif DNA structures are formed in the nuclei of human cells. *Nat Chem*. 2018;10:631-637.
64. Kopylov M, Jackson TM, Stroupe ME. Bulged and canonical G-quadruplex conformations determine NDPK binding specificity. *Molecules*. 2019;24:1988.
65. Noer SL, Preus S, Gudnason D, Aznauryan M, Mergny JL, Birkedal V. Folding dynamics and conformational heterogeneity of human telomeric G-quadruplex structures in Na+ solutions by single molecule FRET microscopy. *Nucleic Acids Res*. 2016;44:464-471.
66. Yoshida W, Saikyo H, Nakabayashi K, et al. Identification of G-quadruplex clusters by high-throughput sequencing of whole-genome amplified products with a G-quadruplex ligand. *Sci Rep*. 2018;8:3116.
67. You J, Li H, Lu XM, et al. Effects of monovalent cations on folding kinetics of G-quadruplexes. *Bioscience Reports*. 2017;37:BSR20170771.
68. Gyimesi M, Harami GM, Kocsis ZS, Kovacs M. Recent adaptations of fluorescence techniques for the determination of mechanistic parameters of helicases and translocases. *Methods*. 2016;108:24-39.
69. Cejka P, Kowalczykowski SC. The full-length Saccharomyces cerevisiae Sgs1 protein is a vigorous DNA helicase that preferentially unwinds holliday junctions. *J Biol Chem*. 2010;285:8290-8301.
70. Lahaye A, Leterme S, Foury F. PIF1 DNA helicase from *Saccharomyces cerevisiae*. Biochemical characterization of the enzyme. *J Biol Chem*. 1993;268:26155-26161.
71. Lerner LK, Sale JE. Replication of G quadruplex DNA. *Genes*. 2019;10:95.
72. Monchaud D, Allain C, Bertrand H, et al. Ligands playing musical chairs with G-quadruplex DNA: a rapid and simple displacement assay for identifying selective G-quadruplex binders. *Biochimie*. 2008;90:1207-1223.
73. Buzovetsky O, Kwon Y, Pham NT, et al. Role of the Pif1-PCNA complex in Pol delta-dependent strand displacement DNA synthesis and break-induced replication. *Cell Rep*. 2017;21:1707-1714.
74. Dahan D, Tsirkas I, Dovrat D, et al. Pif1 is essential for efficient replisome progression through lagging strand G-quadruplex DNA secondary structures. *Nucleic Acids Res*. 2018;46:11847-11857.
75. Garcia-Rodriguez N, Wong RP, Ulrich HD. The helicase Pif1 functions in the template switching pathway of DNA damage bypass. *Nucleic Acids Res*. 2018;46:8347-8356.
76. Liberi G, Maffioletti G, Lucca C, et al. Rad51-dependent DNA structures accumulate at damaged replication forks in sgs1 mutants defective in the yeast ortholog of BLM RecQ helicase. *Genes Dev*. 2005;19:339-350.
77. Myung K, Datta A, Chen C, Kolodner RD. SGS1, the *Saccharomyces cerevisiae* homologue of BLM and WRN, suppresses genome instability and homeologous recombination. *Nat Genet*. 2001;27:113-116.
78. Schmidt KH, Wu J, Kolodner RD. Control of translocations between highly diverged genes by Sgs1, the *Saccharomyces cerevisiae* homolog of the Bloom's syndrome protein. *Mol Cell Biol*. 2006;26:5406-5420.
79. Spell RM, Jinks-Robertson S. Examination of the roles of Sgs1 and Srs2 helicases in the enforcement of recombination fidelity in *Saccharomyces cerevisiae*. *Genetics*. 2004;168:1855-1865.
80. Watt PM, Hickson ID, Borts RH, Louis EJ. SGS1, a homologue of the Bloom's and Werner's syndrome genes, is required for maintenance of genome stability in *Saccharomyces cerevisiae*. *Genetics*. 1996;144:935-945.
81. Schulz VP, Zakian VA. The saccharomyces PIF1 DNA helicase inhibits telomere elongation and de novo telomere formation. *Cell*. 1994;76:145-155.
82. Motegi A, Myung K. Measuring the rate of gross chromosomal rearrangements in Saccharomyces cerevisiae: a practical approach to study genomic rearrangements observed in cancer. *Methods*. 2007;41:168-176.
83. Downs JA, Lowndes NF, Jackson SP. A role for *Saccharomyces cerevisiae* histone H2A in DNA repair. *Nature*. 2000;408:1001-1004.
84. Rhodes D, Lipps HJ. G-quadruplexes and their regulatory roles in biology. *Nucleic Acids Res*. 2015;43:8627-8637.
85. Sabouri N, Capra JA, Zakian VA. The essential *Schizosaccharomyces pombe* Pfh1 DNA helicase promotes fork movement past G-quadruplex motifs to prevent DNA damage. *BMC Biol*. 2014;12:101.
86. Rossi ML, Pike JE, Wang W, Burgers PM, Campbell JL, Bambara RA. Pif1 helicase directs eukaryotic Okazaki fragments toward the

two-nuclease cleavage pathway for primer removal. *J Biol Chem*. 2008;283:27483-27493.

87. Rossi SE, Foiani M, Giannattasio M. Dna2 processes behind the fork long ssDNA flaps generated by Pif1 and replication-dependent strand displacement. *Nat Commun*. 2018;9:4830.
88. Ivessa AS, Zhou JQ, Zakian VA. The Saccharomyces Pif1p DNA helicase and the highly related Rrm3p have opposite effects on replication fork progression in ribosomal DNA. *Cell*. 2000;100:479-489.
89. Rossi SE, Ajazi A, Carotenuto W, Foiani M, Giannattasio M. Rad53-mediated regulation of Rrm3 and Pif1 DNA helicases contributes to prevention of aberrant fork transitions under replication stress. *Cell Rep*. 2015;13:80-92.

SUPPORTING INFORMATION

Additional supporting information may be found online in the Supporting Information section.

How to cite this article: Zacheja T, Toth A, Harami GM, et al. Mgs1 protein supports genome stability via recognition of G-quadruplex DNA structures. *The FASEB Journal*. 2020;34:12646–12662. https://doi.org/10.1096/fj.202000886R